Desalination and Water Treatment
www.deswater.com

10 (2009) 139–143

1944-3994 / 1944-3986

Prediction of ultrafiltration permeate flux decline by means of a shear induced diffusion model with empirical estimation of the gel layer concentration

María-Cinta Vincent-Vela[a], Silvia Álvarez-Blanco[a]*, Jaime Lora-García[a], Enrique Bergantiños-Rodríguez[b]

[a]*Department of Chemical and Nuclear Engineering, Polytechnic University of Valencia, C/Camino de Vera s/n 46022 Valencia, Spain Tel. +34 963877000 Ext. 76383; Fax +34 963877639; e-mail: sialvare@iqn.upv.es*
[b]*Department of Chemical Engineering, Polytechnical Institute José A. Echeverría, Ave. 114, No. 11901, Havana, Cuba*

Received 22 July 2008; Accepted in revised form 23 September 2009

ABSTRACT

In this work, the shear-induced diffusion model has been used to predict flux decline in ultrafiltration. Two types of monotubular ceramic membranes were used in the experiments: Carbosep M2 ZrO_2-TiO_2 membranes with a MWCO of 15 kg/mol (Orelis, S.A., France) and TiO_2–Al_2O_3 Tami MSKT membranes of 5 kg/mol (Tami, S.A., France). Polyethylene glycol (PEG) of 35 kg/mol was used in the preparation of the feed aqueous solution. The experiments were performed at constant temperature (25°C) and at different feed flow rates (1–3 m/s), transmembrane pressures (TMPs) (0.1–0.5 MPa) and feed concentrations (5–15 g/L). In this work the gel layer concentration was empirically estimated form steady-state permeate flux values. Model predictions were compared with the experimental results and discussed. For the Carbosep M2 membranes, model predictions were better for high TMPs and low crossflow velocities. For Tami MSKT membranes, model predictions for initial permeate flux decline were worse when fouling was severe (high TMPs and feed concentrations and low crossflow velocities) than in the case of mild fouling conditions. An explanation for this is given in this paper.

Keywords: Modelling; Ultrafiltration; Gel layer; Polyethylene glycol; Permeate flux decline

1. Introduction

Ultrafiltration is one of the most promising techniques for macromolecular solute separation from aqueous effluents. Nevertheless, the applicability of ultrafiltration is restricted by the fact that permeate flux decreases with time. This phenomenon is commonly termed as membrane fouling [1]. The influence of operating conditions on permeate flux have been widely studied and a wide range of experimental data have been collected and discussed. Despite, more effort has to be done to understand the mechanisms affecting fouling and to develop a model for permeate flux decline with time. Many models have attempted to predict permeate ultrafiltration rate as a function of time for solutions of gel forming polymers. However, all of them fail to accurately predict the behaviour of permeability of ultrafiltration membranes. This work focuses on the shear-induced diffusion model [2,3], which is one of the non-empirical models that achieves better predictions of permeate flux decline with time when compared with other non-empirical models [4–8].

* Corresponding author.

Presented at EuroMed 2008, Desalination for Clean Water and Energy Cooperation among Mediterranean Countries of Europe and the MENA Region, 9–13 November 2008, King Hussein Bin Talal Convention Center, Dead Sea, Jordan.

2. Materials and methods

2.1. Membranes

Two types of monotubular ceramic membranes were used in the experiments: Carbosep M2 ZrO_2-TiO_2 membranes supplied by Orelis, S.A. (France) with a molecular weight cut off (MWCO) of 15 kg/mol and TiO_2–Al_2O_3 Tami MSKT membranes supplied by Tami, S.A. (France) with a MWCO of 5 kg/mol. The membranes area was 35.5 cm^2 and they had an internal diameter of 6 mm.

2.2. Fouling experiments

Polyethylene glycol (PEG) of 35 kg/mol was selected as the feed solute because it has been very often used as a standard macromolecule in fouling ultrafiltration tests carried out for modelling purposes [9,10]. The PEG used in the preparation of the feed aqueous solution was supplied by Merck-Schuchardt (Germany).

The experiments were performed at different feed flow rates (1–3 m/s), transmembrane pressures (TMPs) (0.1–0.5 MPa) and feed concentrations (5–15 g/L). All the experiments were carried out at constant temperature (25°C). Ultrafiltration tests were performed with the ultrafiltration pilot plant described elsewhere [2,4,5].

2.3. Membrane cleaning

Carbosep M2 membrane was cleaned at 40ºC with an aqueous NaOH solution of 0.2% w/w in deionised water. Membrane cleaning procedure for Tami MSKT membrane was carried out with a 0.25 g/L NaOCl aqueous solution at a pH of 11 achieved by NaOH addition. The NaOH and the NaOCl were both supplied by Panreac (Spain). The cleaning protocol managed to recover initial membrane pure water permeability. Consequently, the same membrane was used in all the experiments.

3. Modelling

The shear-induced diffusion model [3] is capable of predicting ultrafiltration permeate flux decline due to gel layer formation and growth with simple equations. The model considers that the growth of the gel layer is governed by the mechanisms of feed-forward filtration. According to the model, for long time scales the tangential flow compensates the convection of solutes towards the membrane surface due to the permeate flow. The tangential flow also prevents the growth of the gel layer and allows achieving a quasi-steady state.

The two main model hypotheses are the following: individual particles collapse with other particles and undergo random displacements from the streamlines and a gel layer adhered to the membrane surface forms instantly from the beginning of ultrafiltration. The main equation of the model has been proposed by Davis [3], who calculated permeate flux, J_P, as a function of time by means of Eq. (1).

$$J_P = \frac{\frac{\Delta P}{\mu \cdot R_m}}{\left(1 + 2 \cdot \beta \cdot \frac{\left(t - \frac{\left(C_{gv} - C_{0v} - C_{0v} \cdot \ln\left(C_g / C_0\right)\right)}{\left(\frac{\Delta P}{\mu \cdot R_m}\right)^2}\right)}{\frac{C_g - C_0}{C_0} \cdot \frac{D_h / 2}{\frac{\Delta P}{\mu \cdot R_m}}}\right)^{-\frac{1}{2}}} \qquad (1)$$

$$\beta = \frac{D_h}{2} \cdot \frac{R_c}{R_m}$$

where ΔP is the transmembrane pressure, μ is the dynamic viscosity of the permeate, R_m is the membrane hydraulic resistance, β is the dimensionless resistance of the cake layer, D is the solute diffusivity, C_{0v} is the solute concentration in the feed expressed in volume per volume, C_{gv} is the solute concentration in the gel layer in volume per volume, C_0 is the feed concentration, C_g is the gel layer concentration, D_h is the hydraulic diameter of the membrane, R_c is the specific resistance of the gel layer and t is time.

The specific resistance of the gel layer can be estimated by means of Eq. (2) [7, 3, 11].

$$R_C = 225 \cdot \frac{(1-\varepsilon)^2}{\varepsilon^4 \cdot a_p^2} \qquad \varepsilon = 1 - C_{gv} \qquad (2)$$

where E is the cake porosity and a_p is the radius of the solute molecule.

The diffusivity of PEG 35 kg/mol at 25ºC was estimated according to the procedure followed by Prádanos et al. [12] and Cheryan [13]. The Stokes-Einstein radius of PEG molecules was estimated according to Möckel et al. [14–16]. The gel layer concentration was empirically estimated from experimental values of steady-state permeate flux J_{Pss} by means of the following equation [17]:

$$\frac{C_g}{C_0} = \exp\left(\frac{J_{Pss} \cdot D_{\text{int}}{}^{0.11} \cdot \upsilon^{0.56}}{0.023 \cdot v_{\text{tang}}{}^{0.89} \cdot D^{0.67}}\right) \qquad (3)$$

where D_{int} is the internal membrane diameter, ν is the kinematic viscosity and v_{tang} is the crossflow velocity. This equation is valid for tubular membranes and turbulent flow.

In this work, the experimental data and the results predicted by the model were compared.

The calculation sequence used to estimate permeate flux decline was the following: Estimation of the gel layer concentration was performed by means of Eq. (3); the estimated value was used for the calculation of the gel layer porosity and the dimensionless specific resistance of the gel layer according to Eqs. (1), (2); finally, the permeate flux as a function of time was obtained by means of Eq.(1).

4. Results and discussion

The shear-induced diffusion model [2,3] is one of the non-empirical models that achieves better predictions of permeate flux decline with time when compared with other non-empirical models [4–8], particularly for the lowest crossflow velocity tested (1 m/s), for which gel layer formation is more likely to occur. To estimate permeate flux, first, the gel layer concentration was empirically calculated by means of Eq. (3). The estimated values of the gel layer concentration were 24.86 g/L for a crossflow velocity of 1 m/s and 24.04 g/L for a crossflow velocity of 3 m/s. Therefore, Eq. (3) predicts that the gel layer concentration slightly decreases as the crossflow velocity increases.

In Figs. 1–6, model predictions with empirical estimation of the gel layer concentration from steady-state permeate flux values [Eq. (3)] are compared with experimental results. The symbols correspond to the experimental results and the continuous lines to those predicted by the model.

In Fig. 1 the best model predictions are attained for the highest TMP tested. Although the shape of the curve for model predictions is similar to that obtained for experimental results, permeate fluxes are over-predicted for low time scales and under-predicted for high time scales when compared with experimental results.

In Fig. 2 it can be observed that model predictions are worse than those observed in Fig. 1. Experimentally observed flux decline with time was very low. Nevertheless, the reduction in permeate flux decline observed when increasing crossflow velocity was higher for the experimental results than in the case of model predictions. In both cases permeate fluxes are over-predicted for low time scales and under-predicted for high time scales.

When the results represented in Figs. 1–2 are compared to those obtained with the same model but with theoretical estimation of the gel layer concentration [2], it can be observed that when the gel layer concentration is empirically estimated the model predicts higher membrane fouling than that predicted when of the gel layer concentration is theoretically estimated. The reason can be the higher value of the gel layer concentration that was obtained when it was empirically estimated. Therefore, empirical estimation of the gel layer concentration does not result in better model predictions.

Comparing Figs.1–2 and Figs. 3–4, it can be observed that for the same operating conditions better predictions are obtained for steady-state permeate flux for Tami MSKT membranes than in the case of Carbosep M2 membranes. The amount of molecules that contribute to the gel layer formation in the case of Carbosep M2 membranes is lower than in the case of Tami MSKT membranes. Retention values for Carbosep M2 membranes with PEG

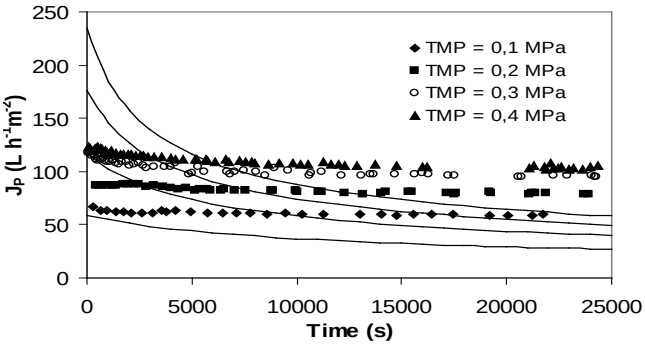

Fig. 2. Experimental data and model predictions for a crossflow velocity of 3 m/s and a feed concentration of 5 g/L for the Carbosep M2 membrane.

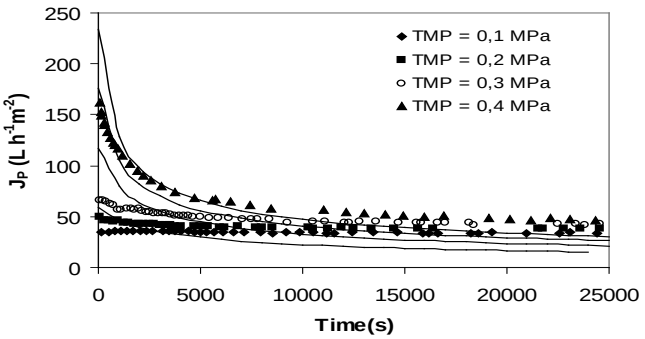

Fig. 1. Experimental data and model predictions for a crossflow velocity of 1 m/s and a feed concentration of 5 g/L for the Carbosep M2 membrane.

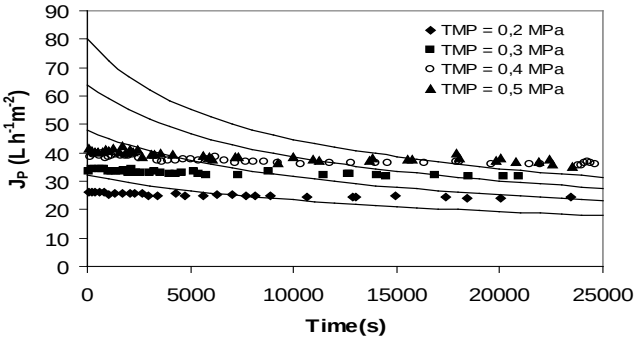

Fig. 3. Experimental data and model predictions for a crossflow velocity of 1 m/s and a feed concentration of 5 g/L for the Tami MSKT membrane.

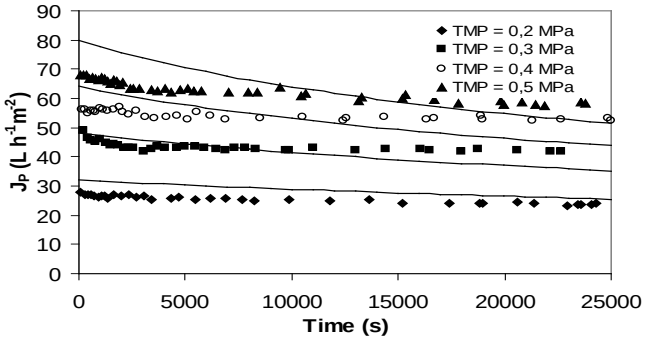

Fig. 4. Experimental data and model predictions for a crossflow velocity of 3 m/s and a feed concentration of 5 g/L for the Tami MSKT membrane.

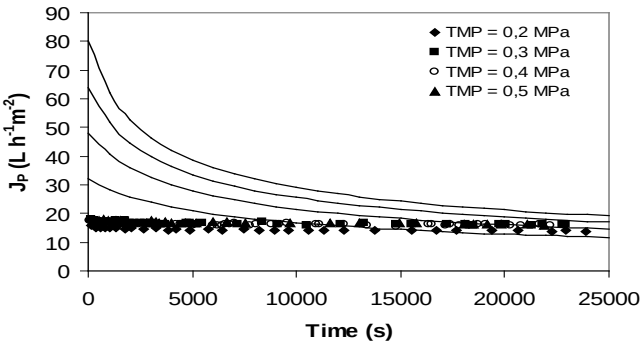

Fig. 5. Experimental data and model predictions for a crossflow velocity of 1 m/s and a feed concentration of 15 g/L for the Tami MSKT membrane.

35 kg/mol were around 86% while values ranging from 90.5% to 99.7% were obtained for Tami MSKT membranes.

The shear-induced diffusion model attains the best predictions for permeate flux decline with time when the Tami MSKT membrane is slightly fouled during the ultrafiltration process (Fig. 4). For those experimental conditions differences between pure water permeate flux and permeate flux obtained for the PEG 35 kg/mol aqueous solution are small. When fouling is severe (Fig. 3), model predictions are worse than in the case of mild fouling conditions. The reason can be that other fouling mechanisms not taken into account by this model can participate in the fouling of the membrane, such as pore blocking. Moreover, pore blocking is more likely to occur at the early stages of the ultrafiltration process, when the highest discrepancies between experimental and predicted flux were obtained.

For the Tami MSKT membrane the best results were obtained for highest crossflow velocity (3 m/s) and the lowest feed concentration (5 g/L) tested (Fig. 4). For that experimental conditions fouling and differences between pure water permeate flux and permeate flux with the feed solution are the lowest.

Figs. 5 and 6 correspond to the results obtained with the highest solute concentration tested (15 g/L). The model predicted a higher initial permeate flux decline for high feed concentrations and for low crossflow velocities (Figs. 3–6). However, this was not experimentally observed for the Tami MSKT membrane. An explanation for this can be found in the assumption that initial permeate flux decline occurred instantly at the beginning of ultrafiltration and it was not experimentally detected. Therefore, predictions corresponding to the more favourable conditions for gel layer formation: high feed concentration and low crossflow velocity (Fig. 5), are not better than those achieved when operational conditions are less favourable for gel layer development (Fig. 6). Nevertheless, steady-state permeate flux predictions were good for the Tami MSKT membrane.

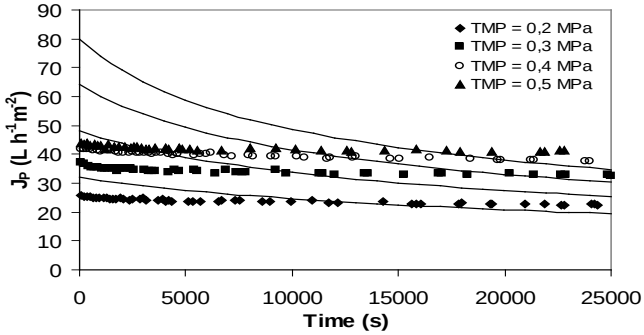

Fig. 6. Experimental data and model predictions for a crossflow velocity of 3 m/s and a feed concentration of 15 g/L for the Tami MSKT membrane.

In all cases, model predictions and experimental results show that the effect of TMP on permeate flux decreases with an increase in TMP and/or feed concentration. However, differences between experimental and predicted results may be due to model assumptions not being correct for all the experimental conditions tested. For example, gel layer formation may not be the only fouling mechanism.

5. Conclusions

Experimental results are not in accordance with model predictions for all the experimental conditions tested.

For the Carbosep M2 membranes, permeate fluxes are over-predicted for low time scales and under-predicted for high time scales when compared with experimental results for all the experimental conditions tested. Moreover, predicted permeate flux with empirical estimation of the gel layer concentration was not better than in the case of theoretical estimation. Model predictions were better for high TMPs and low crossflow velocities for

Carbosep M2 membranes, when gel layer formation is more likely to occur.

However, the opposite was observed with Tami MSKT membranes. When fouling was severe (high TMPs and feed concentrations and low crossflow velocities) model predictions for initial permeate flux decline were worse than in the case of mild fouling conditions. This could be due to an instantaneous initial permeate flux decline that was not experimentally detected. Better predictions were obtained for steady-state permeate flux for Tami MSKT membranes than in the case of Carbosep M2 membranes. An explanation for this can be found in the amount of molecules that contribute to gel layer formation being inferior in the case of Carbosep M2 membranes than in the case of Tami MSKT membranes.

Acknowledgements

The authors of this work wish to gratefully acknowledge the financial support of the Spanish Ministry of Science and Technology (MCYT) through its project no. CTQ2005-03398.

References

[1] C. Bhattacharjee and S. Datta, Analysis of polarized layer resistance during ultrafiltration of PEG-6000: an approach based on filtration theory, Separ. Purif. Tech., 33 (2003) 115–126.

[2] M.C. Vincent-Vela, S. Álvarez-Blanco, J. Lora-García, J.M. Gozálvez-Zafrilla and E. Bergantiños-Rodríguez, Utilization of a shear induced diffusion model to predict permeate flux in the crossflow ultrafiltration of macromolecules, Desalination, 206 (2007) 61–68.

[3] R.H. Davis, Modeling of fouling of crossflow microfiltration membranes, Separ. Purif. Meth., 21 (1992) 75–126.

[4] M.C. Vincent-Vela, S. Álvarez-Blanco and J. Lora-García, Crossflow ultrafiltration of cake forming solutes: a non-steady state model, Desalination, 184 (2005) 347–356.

[5] M.C. Vincent-Vela, S. Álvarez-Blanco, J. Lora-García and E. Bergantiños-Rodríguez, Prediction of flux decline in the ultrafiltration of macromolecules, Desalination, 192 (2006) 323–329.

[6] M.C. Vincent-Vela, S. Álvarez-Blanco, J. Lora-García and E. Bergantiños-Rodríguez, Application of a dynamic model that combines pore blocking and cake formation in crossflow ultrafiltration, Desalination, 200 (2006) 138–139.

[7] M.C. Vincent-Vela, S. Álvarez-Blanco, J. Lora-García and E. Bergantiños-Rodríguez, Application of a dynamic model for predicting flux decline in crossflow ultrafiltration, Desalination, 198 (2006) 303–309.

[8] M.C. Vincent-Vela, S. Álvarez-Blanco, J. Lora-García, J.M. Gozálvez-Zafrilla and E. Bergantiños-Rodríguez, Modelling of flux decline in crossflow ultrafiltration of macromolecules: comparison between predicted and experimental results, Desalination, 204 (2007) 328–334.

[9] S. Ganguly and P.K. Bhattacharya, Development of concentration profile and prediction of flux for ultrafiltration in a radial cross-flow cell, J. Membr. Sci., 97 (1994)185–198.

[10] S. Ghose, C. Battacharjee and S. Datta, Simulation of unstirred batch ultrafiltration process based on a reversible pore-plugging model, J. Membr. Sci., 169 (2000) 29–38.

[11] S. De and P.K. Bhattacharya, Modeling of ultrafiltration process for a two-component aqueous solution of low and high (gel-forming) molecular weight solutes, J. Membr. Sci., 136 (1997) 57–69.

[12] P. Prádanos, J.I. Arribas and A. Hernández, Mass transfer coefficient and retention of PEGs in low pressure cross-flow ultrafiltration through asymmetric membranes, J. Membr. Sci., 99 (1995) 1–20.

[13] M. Cheryan, Ultrafiltration and Microfiltration Handbook. 2nd ed., CRC Press, New York, 1998.

[14] C. Tam and A. Tremblay, Membrane pore characterization — comparison between single and multicomponent solute probe techniques, J. Membr. Sci., 57 (1991) 271–287.

[15] P. Puhlfürβ, A. Voigt, R. Weber and M. Morbe, Microporous TiO_2 membranes with a cut off <500 Da, J. Membr. Sci., 174 (2000) 123–133.

[16] D. Möckel, E. Staude and M.D. Guiver, Static protein adsorption, ultrafiltration behavior and cleanability of hydrophilized polysulfone membranes, J. Membr. Sci., 158 (1999) 63–75.

[17] S. Lee, J. Kim and C.H. Lee, Analysis of $CaSO_4$ scale formation mechanism in various nanofiltration modules, J. Membr. Sci., 163 (1999) 63–74.